

Lateral lithologic distribution of Triassic formations in the Algerian Oued Mya basin using combined petro-elastic and seismic inversion attributes

B. ZEGAGH¹, S. ELADJ¹, A. MIHOUBI², S. BOUFENCHOUCHE³, A. BOULASSEL³, S. GACI⁴, M. FARFOUR⁵, A. KEHILA², M. ARAB² AND K. BENNAMANE²

¹ *Laboratory of Physics of the Earth, University M'Hamed Bougara, Boumerdes, Algeria*

² *Sonatrach Exploration Division, Boumerdes, Algeria*

³ *Sonatrach, Direction of Exploration Operations, Ouargla, Algeria*

⁴ *Sonatrach, Central Directorate of Research & Development, Boumerdes, Algeria*

⁵ *Department of Earth Sciences, Sultan Qaboos University, Al-Khod, Oman*

(Received: 13 October 2024; accepted: 11 March 2025; published online: 20 June 2025)

ABSTRACT This paper presents a combined litho-discrimination approach based on petro-elastic attributes and simultaneous seismic inversion. The analysis adopted attempts to characterise the Triassic fluvial reservoirs, in the Oued Mya basin, Algeria, in terms of lateral distributions of sandstone, shale, and silt. The Triassic sandstones suffer from the presence of silt, which significantly increases the compaction degree of the reservoir parts and decreases the quality of petrophysical properties. The litho-discrimination analysis improves seismic inversion accuracy, providing a more detailed understanding of subsurface rock properties. It separates the effects of different rock types, such as sandstone and shale, leading to better interpretations while reducing noise. It avoids misinterpreting noise as geological signals and, thus, yields more reliable inversion results. It enables better differentiation of complex lithologies, which is particularly crucial in regions with subtle variations in rock properties. For the purpose of an efficient litho-discrimination, a variety of petro-elastic attributes have been carefully examined to find the best attributes that can respond to lithology change. S- and P-impedances are found to be adequate litho-discrimination models with the best prediction capabilities. They have a high correlation coefficient and slightly linear lithology regressions for sand, silt, and shale, showing a good agreement with gamma ray well log responses and analysis results of core data. The litho-discrimination analysis can assist us in the prospect generation and risk assessment of the optimum locations for drilling wells in the region. Seismic pre-stack inversion is used to predict variations away from the well location. The applied workflow enables better discrimination of silt, sandstone, and shale within the T2 reservoir, where the presence of silt is mostly associated with compaction. The seismic analysis revealed a random non-uniform laterally distributed silt over the upper part of the T2 reservoir, which is consistent with the geological and sedimentological descriptions that support the existence and absence of compact intervals from well to well in the studied region. The later compaction (silty levels) is the main possible cause of the petrophysical parameter alteration, resulting in differences in the production results (oil, water, etc.) of the drilled wells in the area of interest.

Key words: seismic, well logs, Trias, T2 reservoir, petro-elastic, lithology prediction, pre-stack simultaneous inversion, impedance, and litho-discrimination.

1. Introduction

Reservoir characterisation is a broad term encompassing various methods and techniques to determine the physical properties of a reservoir, such as lithology, thickness, porosity, and channels (Farfour *et al.*, 2012) and their distribution within the reservoir (Sheriff, 2002; Slatt, 2006). The choice of techniques and their efficiency largely depend on the availability of data and the geological challenges to be addressed (Filippova *et al.*, 2011; Onajite, 2021). Seismic-based techniques have been widely used for lithology prediction (Avseth *et al.*, 2005; Arpaci and Ramachandran, 2013; Chen *et al.*, 2015; Farfour *et al.*, 2015; Yenwongfai *et al.*, 2016; Amoura *et al.*, 2022; Zrelli *et al.*, 2023), with seismic inversion emerging as a reliable and accurate method for lithological reservoir characterisation (Durrani *et al.*, 2022; Zrelli *et al.*, 2023).

Oued Mya is among the most important and productive basins in Algeria. By 2005, exploration in the area revealed that only 2 out of 15 oil wells were successful in the Triassic sandstones, specifically in the upper (T2) and the lower (T1) Triassic formations. In 2014, after multiple attempts, the Algerian petroleum company Sonatrach made a hydrocarbon discovery at the W-4 well, renewing interest in the Triassic reservoirs. Since then, exploration efforts have focused primarily on this target.

Despite progress, significant challenges persist. One major issue is the discrepancy in well productivity, even within short distances. For example, wells located 4.5 km apart showed stark differences: one produced hydrocarbon while the other was dry. Similar inconsistencies were observed in other structures, such as the Hassi Boukhellala Nord well, where W-5 encountered oil, but W-6, drilled 6 km away, was dry. Petrographic analyses revealed that the T2 reservoir is characterised by dolomite and anhydritic cement, which significantly reduce petrophysical properties. Permeable intervals in the T2 reservoir range from 100 to 700 md, with porosities between 11% and 20%. These are interspersed with compact intervals, where permeability drops to 0.02-8 md and porosity ranges from 2% to 9%. Previous seismic efforts consistently failed to support the sedimentological model, leading to the recommendation of seismic inversion techniques for improved characterisation (Bennamane *et al.*, 2016).

Data have shown that the Triassic sandstones are remarkably affected by the presence of silt, which reduces or completely closes the pores. This phenomenon is observed, in particular, in the upper part of the T2 reservoir, which is often very compact.

Since 2012, advances in data acquisition, including 3D seismic surveys, well logging, core analysis, and petrographic studies, have provided new insights. Bennamane *et al.* (2016) used the above data sets to confirm the significant impact of lithological variability. In contrast to the previous studies that described the depositional environment in the region of interest as a braided fluvial channel for the T2 sandstone, Bennamane *et al.* (2016) demonstrated that the environment is of a meandering type and recommended seismic inversion as a potential tool to find interpretation for the discrepancy between wells.

This study aims to address above challenges by developing a litho-discrimination approach that integrates petro-elastic analysis, seismic inversion attributes, and rock physics (Russell, 2014; Simm *et al.*, 2014; Mavko *et al.*, 2020). The objective of the approach is to predict the lateral distribution of sandstone, silty sandstone, and shale in the T2 reservoir. The 3D-ATKS seismic data used in the study were recorded in 2014 and purposely processed for pre-stack simultaneous inversion, which was conducted in 2015 for possible lithology prediction. Another objective of the study is to optimise well placement while reducing exploration risks.

2. Geologic setting

2.1. Location of the Oued Mya basin

The Oued Mya basin is located in the northern part of the Algerian Sahara platform (Fig. 1a), approximately 600 km to the south of the Algerian capital (Zerroug *et al.*, 2007). It is composed of several large areas, such as Ghardaïa (Fig. 1b), one of the most productive perimeters, with several blocks. The main area of interest is located in the block 422 (Fig. 1c).

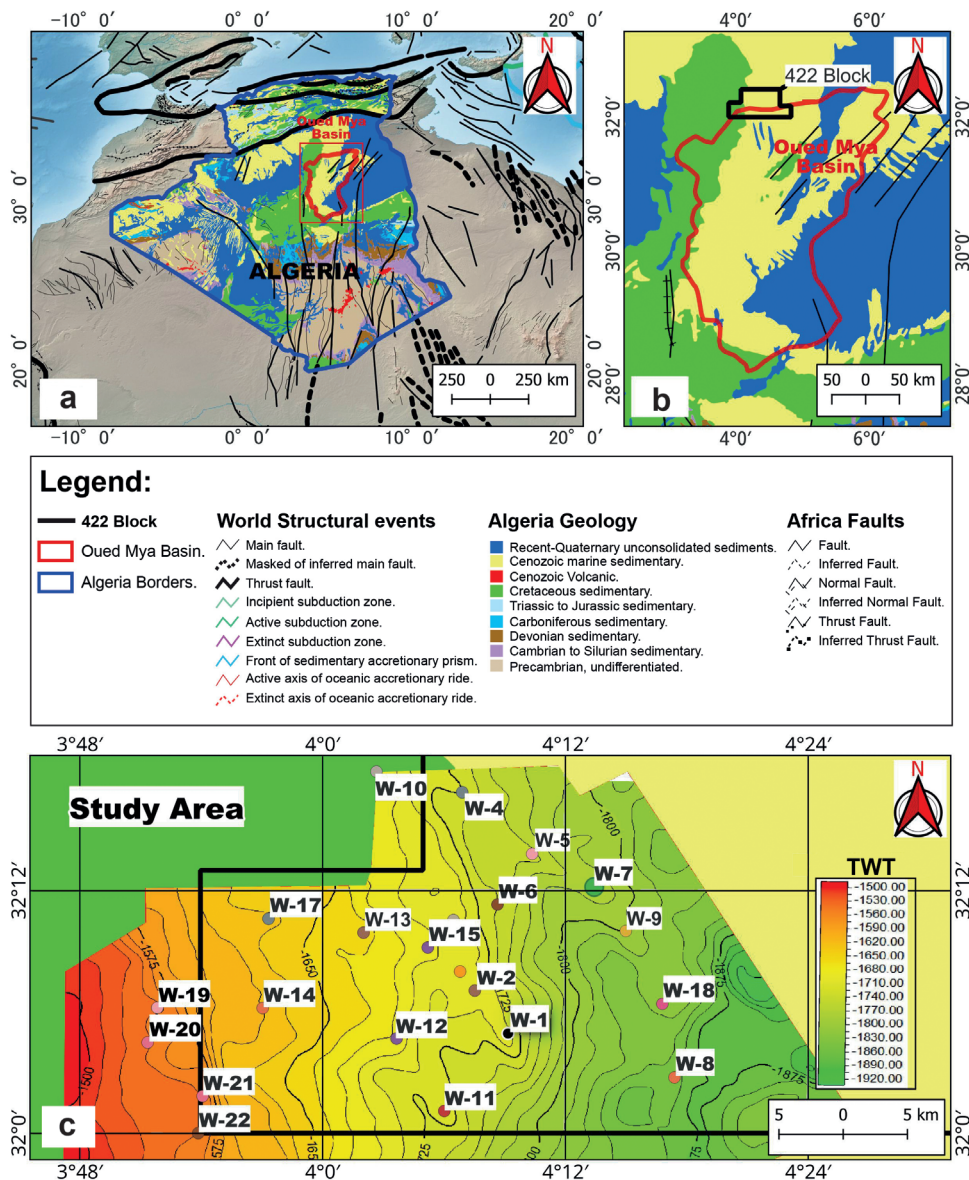


Fig. 1 - Geographic setting of the study area: a) geographic setting of the Oued Mya basin in Algeria, with categories representing major geological units; b) location of the area of interest in the Oued Mya basin; c) well positions displayed on an isochrone map that highlights the structural features (modified after <https://portal.onegeology.org/OnegeologyGlobal/>).

2.2 Stratigraphy and sedimentary environment

The Trias, the first Mesozoic play in the area of interest, consists of six lithological units. From bottom to top, these are: the lower series, the eruptive rocks, level T1 (units B and C), level T2 (unit A), the lower clays, and salt-bearing S4 that unconformably overlies the Ordovician play (Hercynian Orogeny) and conformably underlies the Jurassic play (Zerroug *et al.*, 2007). The average thickness of the Triassic interval, based on six wells, is approximately 160 m across the study area (Fig. 2).

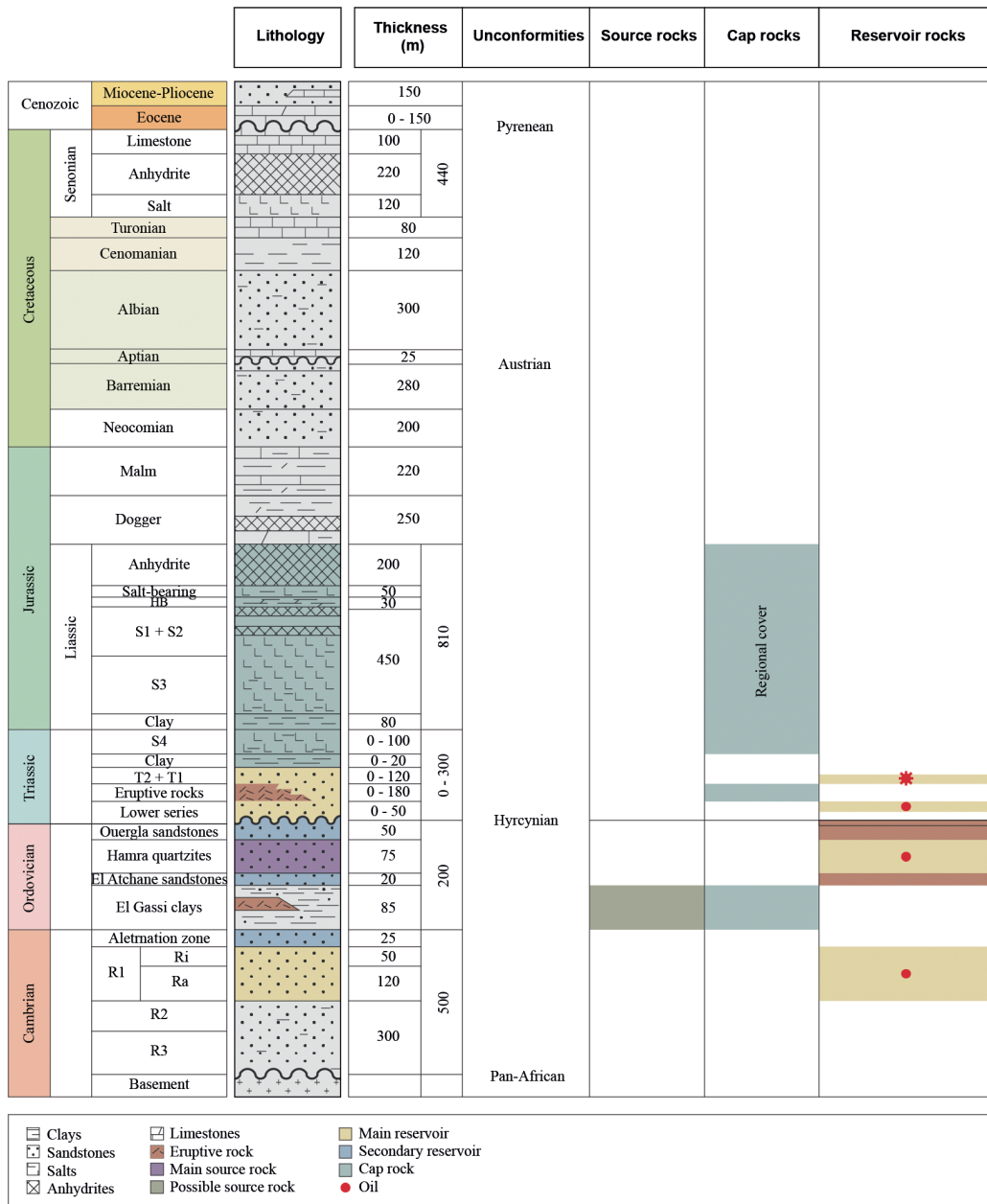


Fig. 2 - Lithologic column for the study area, the Oued Mya basin (Zerroug *et al.*, 2007).

The Triassic sandstone levels were deposited in a continental fluvial environment characterised by lateral variations in lithology and thickness, which are difficult to predict (Zerroug *et al.*, 2007). These reservoirs are significantly affected by compaction and, in some cases, by salt cementation at the top of the T2 unit. The upper part of T2 has been considerably compacted and has been interpreted as a silt level. In certain instances, the upper part of T1 is predominantly composed of silt. Compaction and silt content, two interrelated factors, have a significant impact on petrophysical parameters. However, a recent study by Bennamane *et al.* (2016) demonstrates that the depositional environment is meandering rather than braided, as previously assumed (Fig. 3).

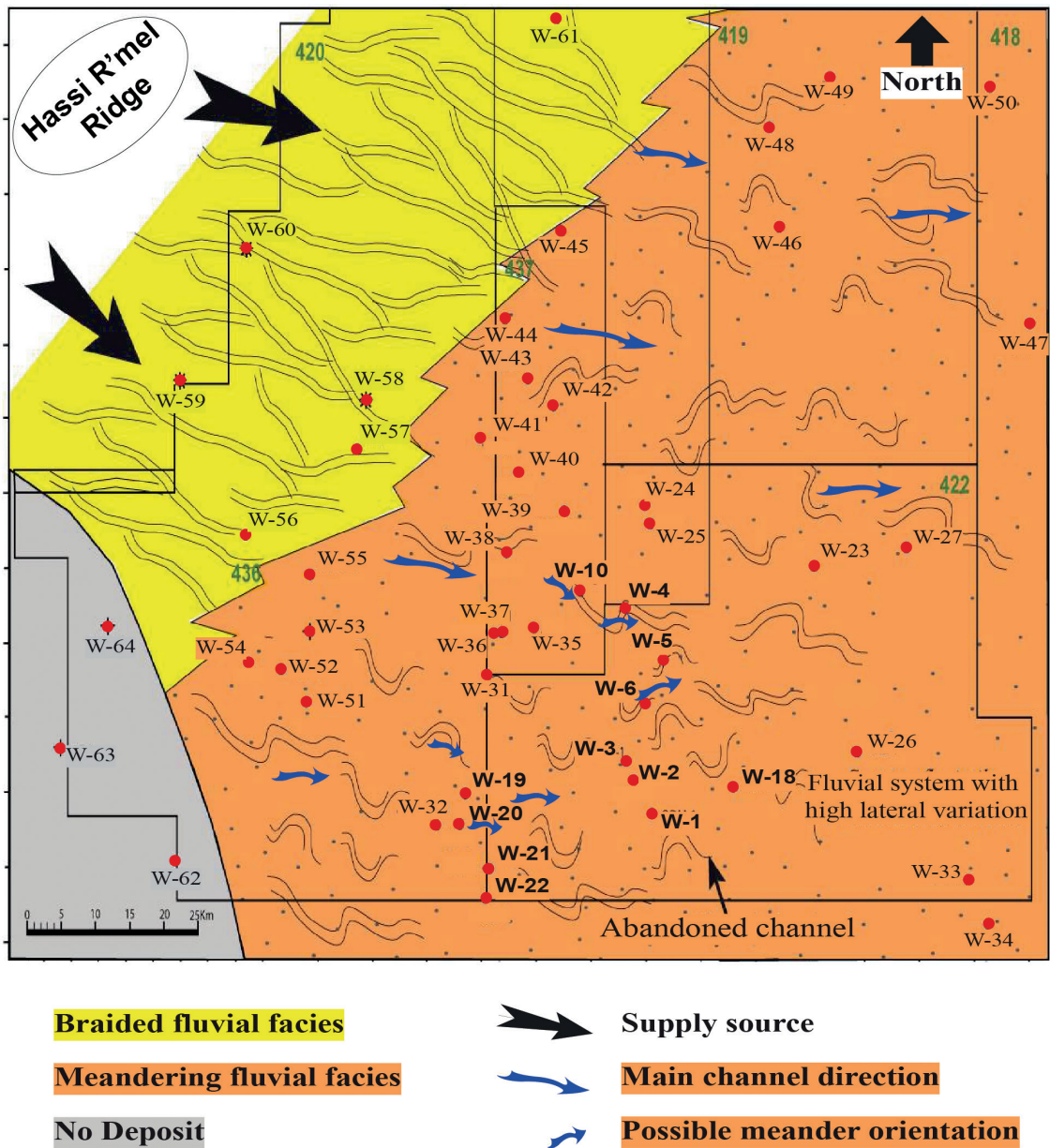


Fig. 3 - Deposition distribution map of the Triassic T2 reservoir in the area of study, the Oued Mya basin (Bennamane *et al.*, 2016).

2.3. Reservoirs

This study focuses on the Triassic T1 and T2 reservoirs. These are the main oil-bearing reservoirs in the region. The average reservoir thickness for T1 and T2 is around 100 m and increases towards the north, where it can exceed 200 m (Zerroug *et al.*, 2007).

Table 1 presents the porosity and permeability values for the Triassic play and its associated reservoirs (T1 and T2).

Table 1 - Porosity and permeability of Triassic reservoir units (Bennamane *et al.*, 2016).

Level/Properties	Average porosity (%)	Average permeability (md)
T2 upper part	5	<10
T2 lower part	>10	100
T1	16	20–2000
Triassic play	15	>200

Grain size analysis indicates that the T2 reservoir is composed of fine- to very fine-grained sandstone, predominantly silty, with clay pebbles and thin silty clay layers, as observed in multiple thin sections from different depths and wells. Lamination types vary from planar to oblique.

Fig. 4 shows a gamma ray (GR) log section of some wells. The section crosses from NW to SE throughout the study area, with the top of the T2 flattened and highlighted in blue. Sandstone intervals are illustrated with yellow-filled GR curves. Overall, the lateral thickness continuity of the T2 reservoir, from north to south, is highly variable. It does not follow a uniform variation

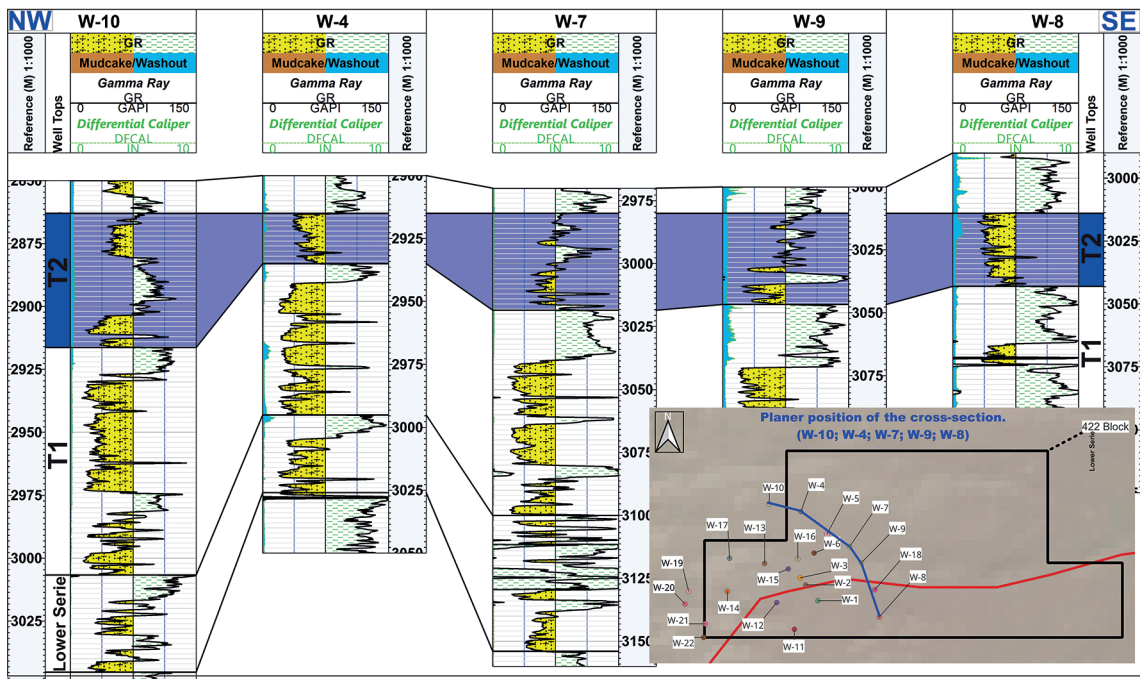


Fig. 4 - GR correlation panel of several wells in the area (NW-SE) showing indications of channelling.

law. Some wells, such as W-4 and W-8, have developed consistent sand bars (T2), while others, W-7 and W-9, have not.

3. Data pre-conditioning and analysis

3.1. Data preconditioning

The seismic data set (Fig. 5) was acquired in October 2012, and amplitude-preserving processing was conducted in 2014 for pre-stack simultaneous inversion.

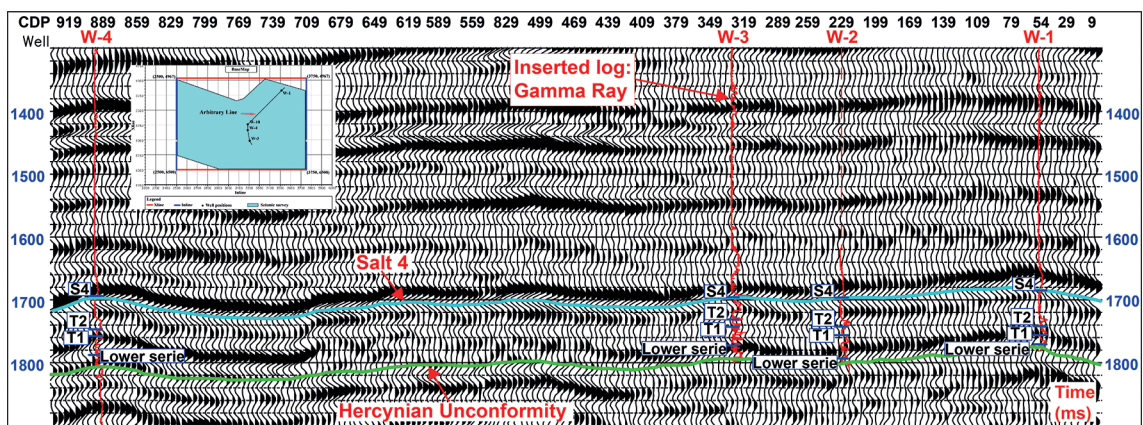


Fig. 5 - Section passing through wells showing the used seismic data. The overlaid red curves on the section represent the GR logs.

To analyse the variation in seismic amplitude with the angle of incidence, the seismic data must be converted into angle stacks (partial stacks). This enables the study of amplitude variation from small-angle data (near offset) to wide-angle data (far offset). Significant variations between the different angle stacks can provide insights into the reservoir contents. The normal-incidence stack primarily reflects information about the matrix (lithology), while the wide-angle stack can offer indications about the reservoir contents.

Three angle stacks, covering different ranges of incidence angles (0° - 13° , 13° - 24° , and 24° - 35°), have been generated to characterise the Triassic reservoirs (Figs. 6 to 8).

It is worth noting that the data were processed using amplitude-friendly processing so that they could be exploited for lithologic and stratigraphic interpretation purposes (Farfour and Yoon, 2014; Farfour and Foster, 2022). The processing sequence applied is outlined in Table 2.

Well data have been integrated and listed in Table 3. These include core measurements and descriptions, petrographic analysis, master logs, drilling stem test (DST), fluid sampling and logging data (Table 3), as well as GRs (GR), calliper (Cal), electrical resistivity logging (R), bulk density logging (RHOB), neutron porosity logging (NPHI), corrected bulk density (DRHO), photoelectric absorption factor (PEF), compressional slowness logging (DTC), shear slowness logging (DTS), spectrometry logs (thorium, potassium, and uranium), etc. (Fig. 9).

Some well logs exhibit poor quality, inconsistencies with neighbouring wells, and/or missing

Table 2 - Seismic data processing sequence.

Steps	Process	Description
1	Data reading	SEG-D data with a length of 4.0 s and a sample rate of 4 ms; data conversion from SegD to internal format
2	Geometry quality control (QC) and assignment	Data labelling with surface geometry Information followed by check and quality control
3	Static application	Elimination and correction of weathering zone effect for datum plane
4	Despiking	Applied to both shot and receiver domains
5	Spherical divergence correction	Compensation for spherical divergence amplitude attenuation
6	Random and linear noise attenuation	Multi-domain noise attenuation
7	Minimum-phase conversion	Deconvolution preconditioning
8	Surface-consistent predictive deconvolution	GAP: 24 ms, operator length: 160 ms
9	Zero phase conversion	Velocity picking preconditioning
10	First velocity analysis	Conducted on a grid of 1.0×1.0 km ²
11	Surface-consistent residual statics	Alignment of traces within common midpoint (CMP) gathers
12	Second velocity analysis	Conducted on a grid of 1.0×1.0 km ²
13	Surface-consistent residual statics	Re-applied for enhanced precision
14	Surface-consistent amplitude correction	Compensation of special amplitude variations
15	Despiking on common depth point (CDP) domain	Removal of residual noise on the CDP domain
16	Fourier regularisation on XSpread domain	Smoothing and regularisation of amplitude in the Fourier domain
17	Full 3D Kirchhoff pre-stack time migration	Migration of seismic data to correct reflector positioning
18	Multiple attenuation	Velocity discrimination and radon domain multiple attenuation
19	Normal moveout (NMO) application	Correction of NMO to flatten reflection events within CMP gathers
20	Mute	Stretch effect suppression
21	Partial angle stack generation	Delivery of partial angle stack after offset to angles conversion
22	Full 3D stack	Summing of traces to enhance signal-to-noise ratio
23	Footprint amplitude attenuation	Reduction of acquisition footprint effects
24	Output	Final processed data exported in SEG-Y format; gather, stack and velocity deliverables

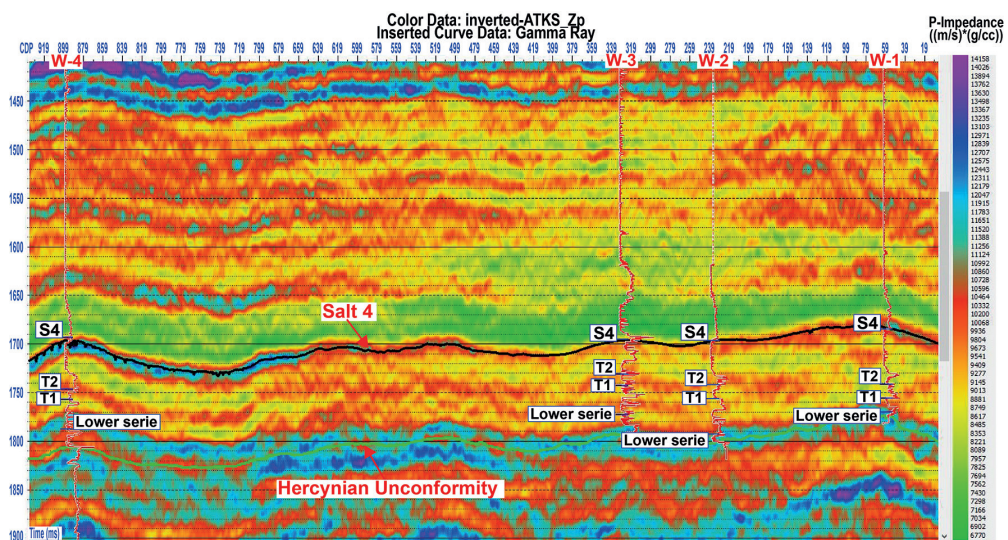


Fig. 6 - Section passing through wells showing the inverted acoustic impedance (Zp). The overlaid vertical red curves on the section represent the GR logs.

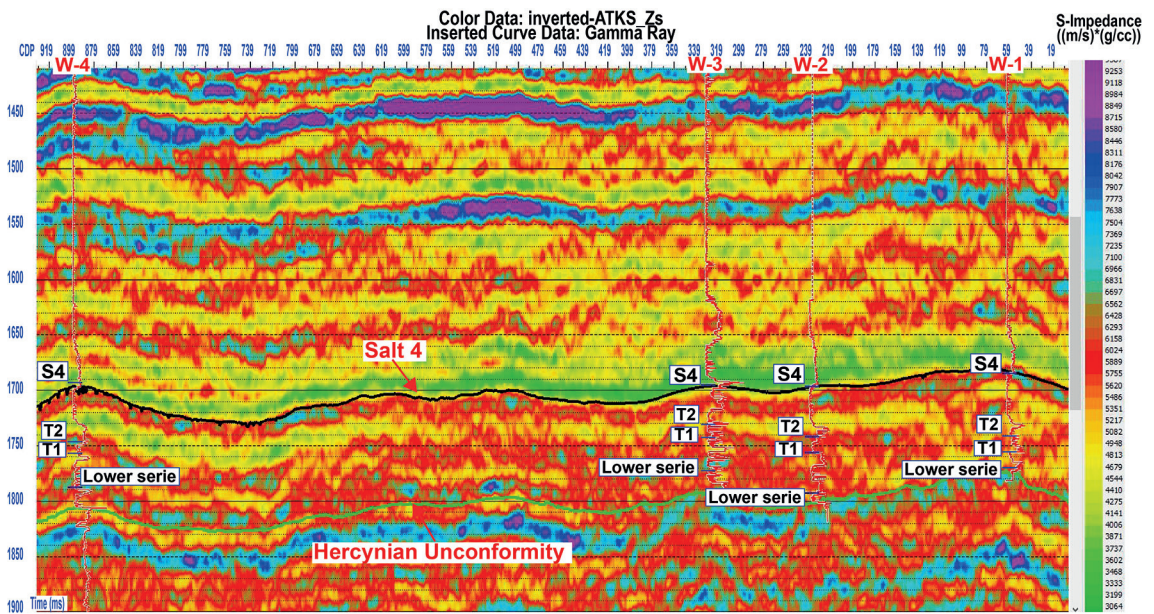


Fig. 7 - Section passing through wells showing the inverted acoustic impedance (Zs). The overlaid vertical red curves on the section represent the GR logs.

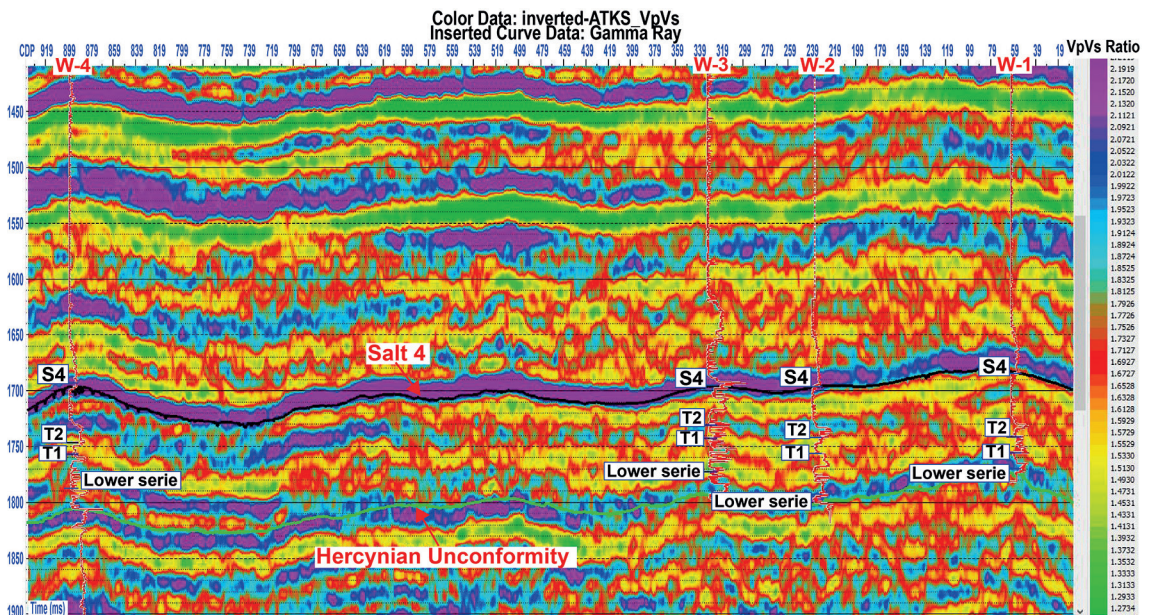


Fig. 8 - Section passing through wells showing the inverted VpVs ratio. The overlaid vertical red curves on the section represent the GR logs.

sections or trends. To address these issues, well log conditioning was applied prior to integrating the logs with seismic data (Gunarto and Irawan, 2010). This process involves data normalisation for adjusting well log measurements to a common scale or reference. By plotting each log versus depth to establish a trend, data values that deviate significantly from this trend are considered

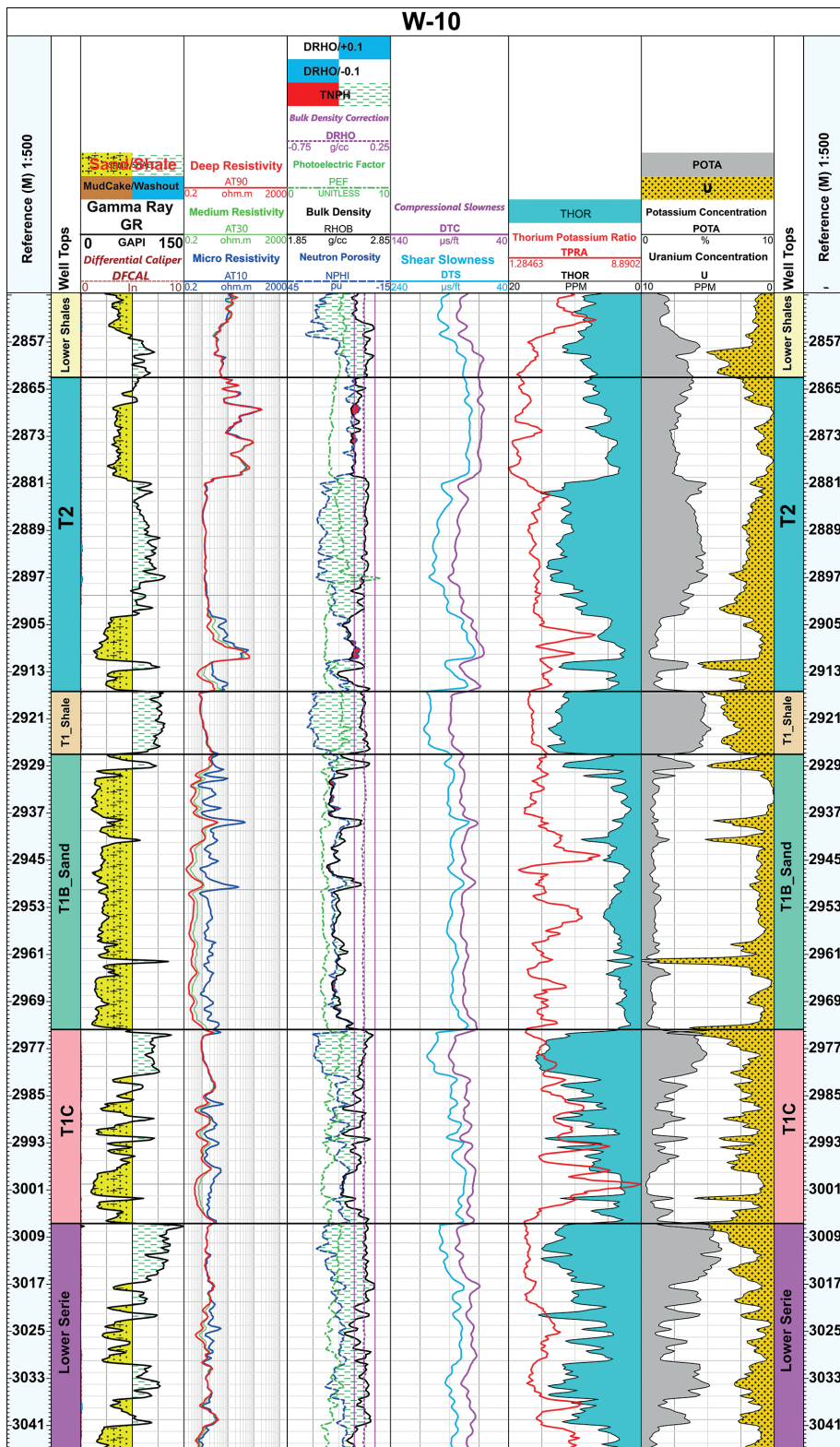


Fig. 9 - Petrophysical logs for the Triassic play. Logs from left to right: GR, R, NPHI, RHOB, DTC, DTS, thorium, potassium, and uranium (W-10).

outliers and are edited appropriately. Noise reduction is also performed to eliminate random errors and noise from the data. The generation of missing log segments, as well as other corrective actions, has been implemented (Anderson *et al.*, 2008; Al Shekaili *et al.*, 2012; Cannon, 2015).

Table 3 - Checklist of various logs, recorded from the wells in the area of study.

Well	GR	Cal	R	RHOB	NPHI	DRHO	PEF	DTC	DTS	Spectrometry
W-1	✓	✓	✓	✓	✓	✓	✓	✓	✗	✓
W-2	✓	✓	✓	✓	✓	✓	✓	✓	✗	✓
W-3	✓	✓	✓	✓	✓	✓	✓	✓	✓	✓
W-4	✓	✓	✓	✓	✓	✓	✓	✓	✓	✓
W-5	✓	✓	✓	✓	✓	✓	✓	✓	✗	✓
W-6	✓	✓	✓	✓	✓	✓	✓	✓	✓	✓
W-7	✓	✓	✓	✗	✗	✗	✓	✓	✓	✓
W-8	✓	✓	✓	✓	✓	✓	✓	✓	✗	✓
W-9	✓	✓	✓	✓	✓	✓	✓	✓	✓	✓
W-10	✓	✓	✓	✓	✓	✓	✓	✓	✓	✓
W-11	✓	✓	✓	✓	✓	✓	✓	✓	✗	✓
W-12	✓	✓	✓	✓	✓	✓	✓	✓	✗	✓
W-13	✓	✓	✓	✓	✓	✗	✓	✓	✓	✓
W-14	✓	✓	✓	✓	✓	✓	✓	✓	✗	✓
W-15	✓	✓	✓	✓	✓	✓	✓	✓	✓	✓
W-16	✓	✓	✓	✓	✓	✓	✓	✓	✓	✓
W-17	✓	✓	✓	✓	✓	✓	✓	✓	✓	✓

3.2. Data analysis

Multiple histograms/cross-plots were performed to analyse the used well data (Fig. 10).

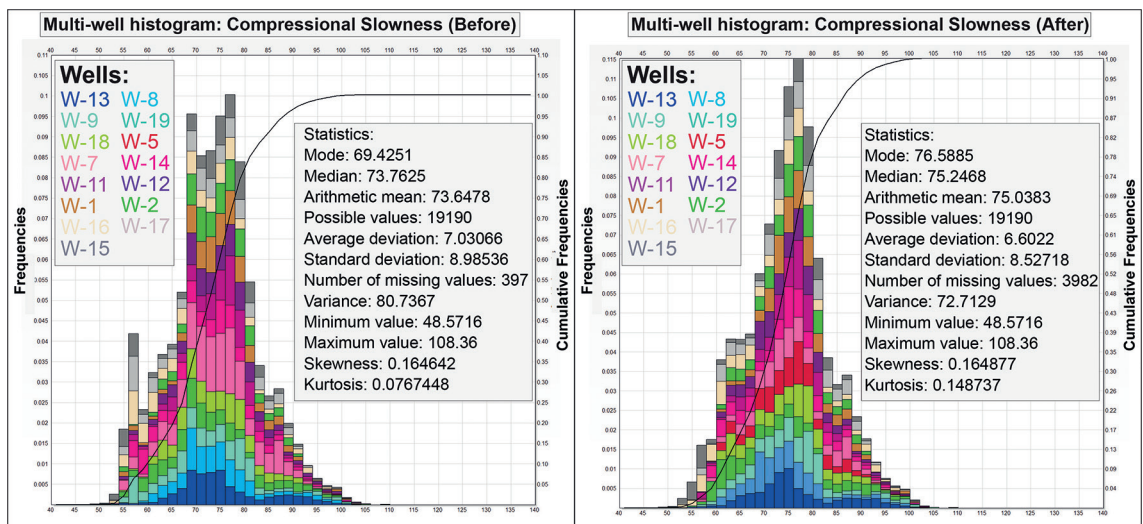


Fig. 10 - Example histogram for a multi-well case, highlighting DTC log data preconditioning from 15 wells.

The data were analysed to assess their uniformity and to detect any abnormalities or outliers. For this purpose, histograms have been generated for all the available logs including DTC, DTS, and RHOB. The histograms showed that the data are well distributed and no outliers are observed (Fig. 10).

4. Methodology

The methodology used is primarily based on simultaneous seismic inversion (Russell, 1988; Hampson *et al.*, 2005; Pendrel, 2006; Russell and Hampson, 2006) and their derived attributes to perform litho-discrimination of Triassic reservoirs. Multiple petro-elastic attributes have been thoroughly examined to identify the ones that are most sensitive to the targeted lithology and yield the best lithology discrimination models. The best models should exhibit discernible trends with minimal overlap and scattering, ensuring optimal separation. The employed models need to be correlated with the GR for lithology validation. Core data descriptions have been included to confirm the prediction of sandstone, silty sandstone, and shale based on the selected attributes. Additionally, they are used to assess the effectiveness of these attributes in distinguishing the targeted lithologies (sandstone, silty sandstone, and shale). To predict the lithological behaviour away from the well location, the seismic inverted data have been used to interpolate the elaborated knowledge (petro-elastic relationships) at the well over the whole area of interest. To reinforce the study, recent wells have been quality conditioned for petro-elastic evaluation and integrated to revalidate the applied approach. The predicted and obtained lithological results have been found to be consistent (Fig. 11).

Fig. 11 illustrates a workflow of the phases completed during the realisation of this work. The workflow begins with a seismic pre-stack inversion to extract the seismic attributes. Concurrently, a petro-elastic analysis has been conducted to integrate additional wells and establish attribute relationships at well locations for litho-discrimination. Based on the seismic inversion attributes, the outcomes of the litho-discrimination analysis will be used to predict and extrapolate the spatial distribution of the various targeted facies (sandstone, shale, and silt) from the seismic data (P-impedance and S-impedance).

5. Results and discussion

The approach adopted was implemented in four phases:

- 1) petro-elastic well data analysis;
- 2) attribute analysis for optimal litho-model discrimination;
- 3) well and core data lithology discrimination;
- 4) seismic lithology discrimination.

5.1. Petro-elastic well data analysis

For an efficient attribute analysis, a detailed petrophysical evaluation of the well-log data has been carried out. This includes the petrophysical evaluation of reservoir and elastic properties, as well as the investigation of any possible relationships between them (Xu and Chacko, 2008; Oyetunji, 2013). A good match between calibrated logs and measured core data was achieved (Fig. 12).

Following the results obtained from the petro-elastic study, sandstone levels are highlighted with

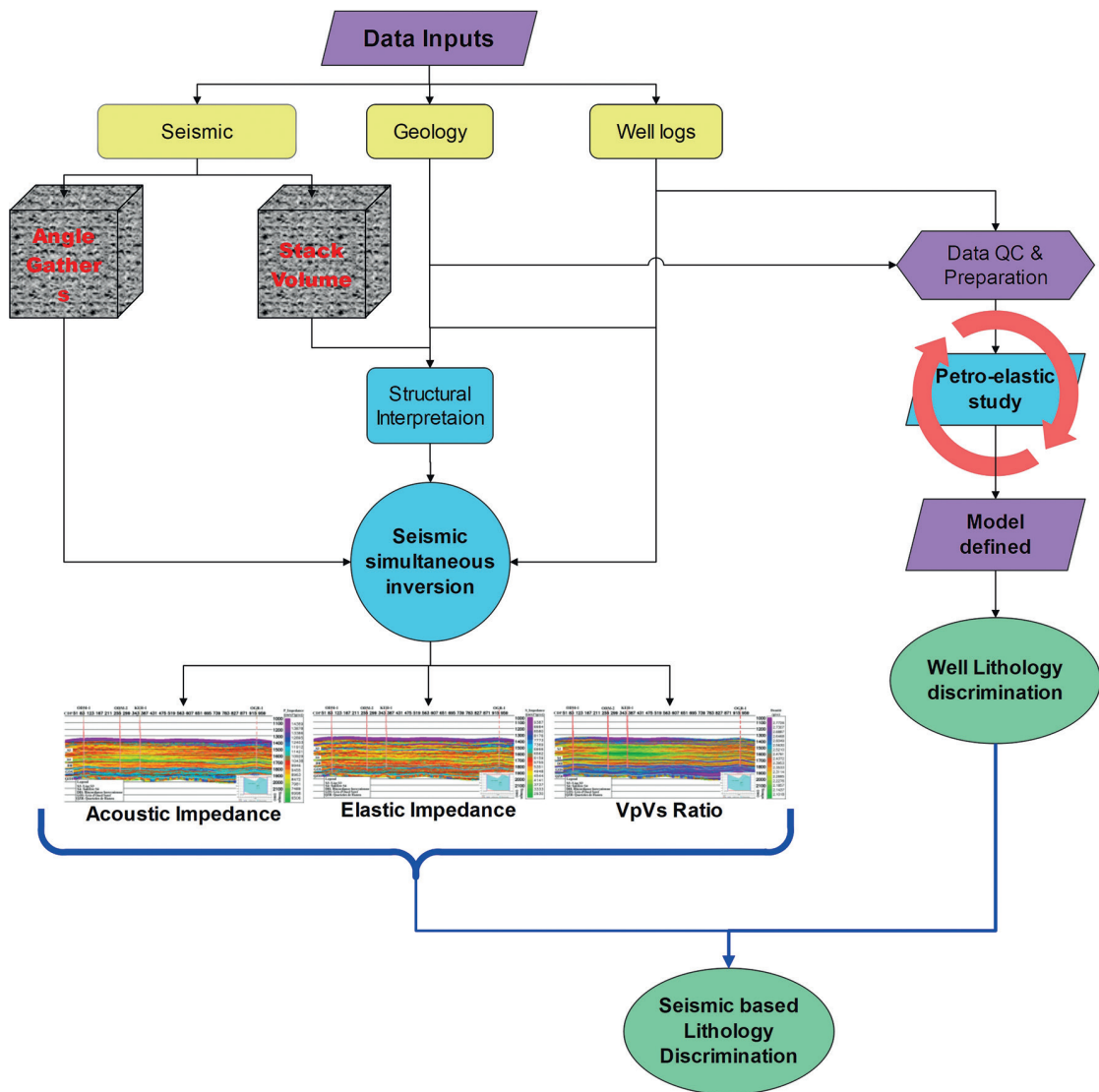


Fig. 11 - Workflow for the adopted methodology.

yellow colour-filled curves corresponding to zones with $V_{sh} < 0.35$ and $V_p/V_s < 1.8$. The RHOB, NPHI, and permeability values, calibrated to core data measurements, are indicated with black, green, and blue dots, respectively. The red arrows indicate the upper and lower parts of the T2 reservoir.

5.2. Attribute analysis for the best litho-model discrimination

This paragraph illustrates the attributes that have been chosen to generate the best models. These models have been constructed by examining almost all of the attributes available and their behaviour with respect to sandstones, shale, and/or silt. To determine which attributes are the most sensitive to lithology, many petro-elastic cross-plots have been generated, calibrated with GRs, and correlated with core data measurements. Some criteria have been considered

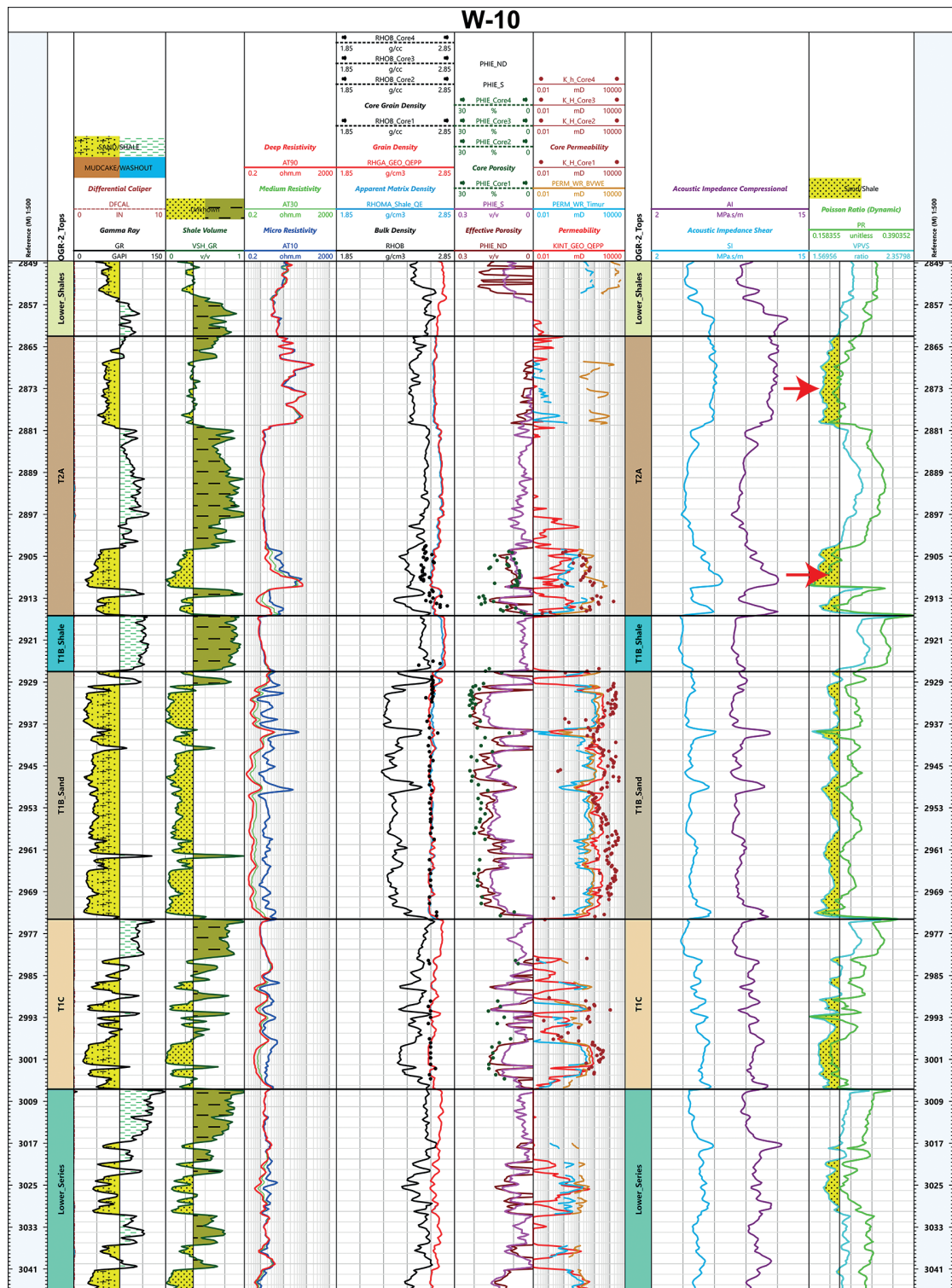


Fig. 12 - Petro-elastic study results of T1 and T2 reservoirs from well (W-10). The figure comprises eight columns, presented from left to right: 1) GR log, 2) shale volume, 3) resistivity curves, 4) density logs with core-measured density, 5) porosity logs with core-measured porosity, 6) estimated and core permeability, 7) acoustic and elastic impedances, and 8) Vp/Vs ratio alongside Poisson's ratio.

in the current investigation to assess the effectiveness of the derived models, based on the overlapping, clear separation between the different lithology clusters, and scattering degree (Fig. 13).

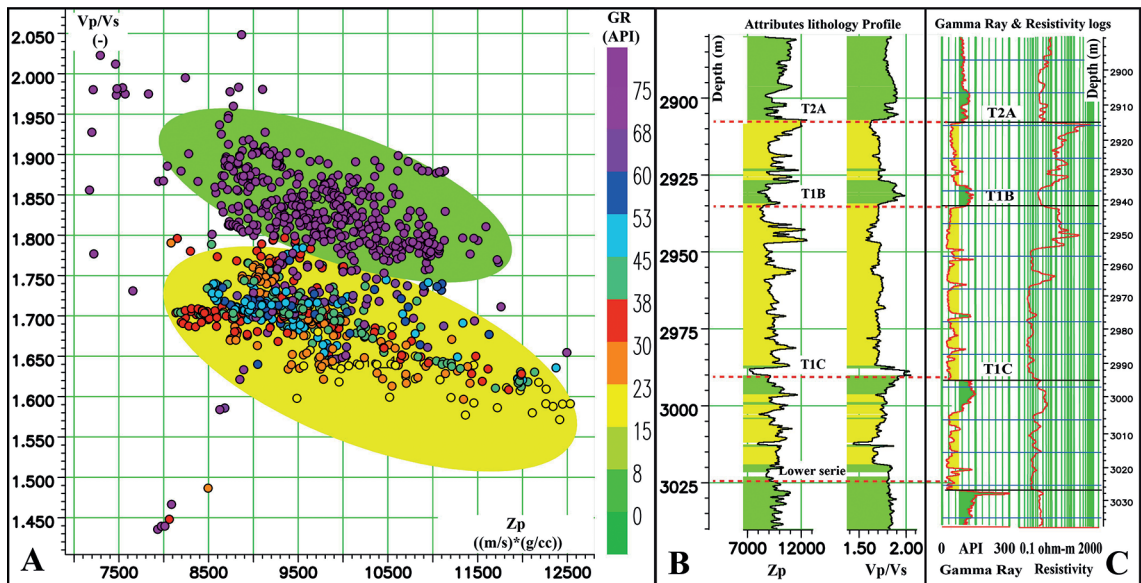


Fig. 13 - A) V_p/V_s ratio versus P-impedance sandstone lithology is colour coded in a yellow ellipse with GR < 75 API, and shale lithology is colour coded in a green ellipse with GR > 75 API in the cross-plot. B) Attribute lithology profile includes a vertical representation of the cross-plot findings. C) The measured GR and R of the analysed well, W-4.

Many models have been rejected for several reasons, among which scattering samples and overlapping levels. However, some models showed effective lithology discrimination. In fact, the P-impedance versus S-impedance cross-plot yields satisfactory discrimination (Fig. 14A). The cross-plot reveals two distinct trends: a clear separation between sandstones and shales, with less scattering, and minimal overlap, leading to the smallest amount of uncertainty in identifying lithology types from seismic data. The coloured ellipses in Fig. 14A highlight lithology clusters, where sandstones (yellow) and shales (green) are well distinguished. Fig. 14B links impedance values to depth, confirming lithological boundaries, while Fig. 14C reinforces the classification through the GR log.

5.3. Well and core data lithology discrimination

After achieving the most appropriate models, a validation stage has been performed with GR and core measured data. Two discrimination phases have been conducted: the first over all the Triassic formations to distinguish sandstone from other lithologies (Fig. 14), and the second to differentiate sandstone from silty sandstone and shale within the T2 reservoir (Fig. 15).

Good correlations have been observed from the comparison of the S-impedance versus P-impedance cross-plot with the GR log plot (Figs. 14B and 14C) and core data (Figs. 15B and 15C).

In Fig. 14A, two distinct lithologies are shown: sandstones with a yellow circle and shales with a green circle. These show two distinct linear trends with good correlation and distribution.

Sandstones exhibit acoustic impedance values ranging from 8500 to 12500 m/s × g/cc, and elastic impedance values ranging from 5000 to 8000 m/s × g/cc, with GR less than 60 API (yellow cluster), whereas shale (green cluster) exhibit GR greater than 75 API.

A good litho-discrimination is well observed in Fig. 14B (impedance logs) and Fig. 14C (GR log).

For more accurate litho-discrimination over the T2 reservoir, core data have been integrated. This was quite useful in distinguishing sandstone from silty sandstone and shale.

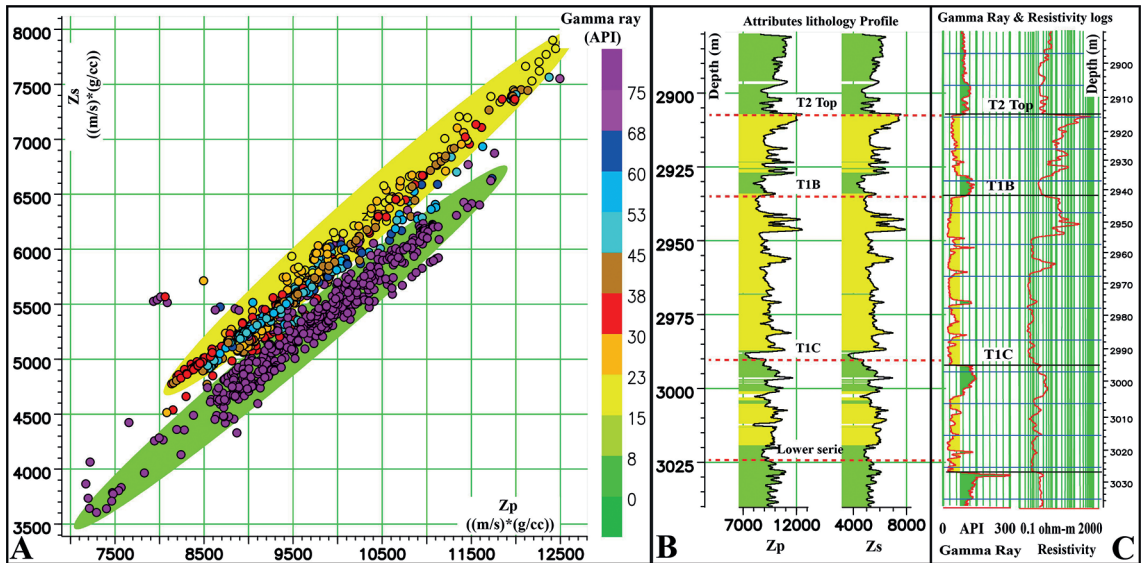


Fig. 14 - A) S-impedance vs P-impedance cross-plot as an example of lithology classification in the elastic domain across all Triassic formations. B) Z_p and Z_s impedance logs. C) The measured GR and resistivity of the studied well, W-4.

Instead of the two previous observed lithologies, the T2 reservoir comprises three lithologies: sandstone, silty sandstone (compact), and shale distributed on two distinct trends (Fig. 15A), with sandstone and silty sandstone following the same trend. Silty sandstone exhibits high impedances (higher than 11500 m/s × g/cc for Z_p and 6750 m/s × g/cc for Z_s) (Fig. 15A). Shales exhibit a different range, with low values for both Z_p and Z_s impedances (green ellipse). A good litho-discrimination is well observed in Fig. 15B (impedance logs) and Fig. 15C (core data). To conclude, the T2 reservoir is silty (compact) at the top, sandy in the middle, and shaly at the bottom (Fig. 15).

5.4. Seismic lithology discrimination

Seismic inversion attributes have been used to discriminate the different lithologies away from the wells. Following the same strategy, and using seismic simultaneous inversion deliverables, acoustic and elastic impedances, a lateral prediction of the sandstone, silty sandstone, and shale distributions have been carried out (Figs. 16 and 17). The litho-discrimination of sandstones from other lithologies, over all Triassic formations, reveals distinct distribution of sandstones and shales (Figs. 16A and 16B). When considering only the T2 reservoir parts, three lithologies have been identified: sandstone, silty sandstone, and shale (Figs. 17A and 17B). A similar litho-

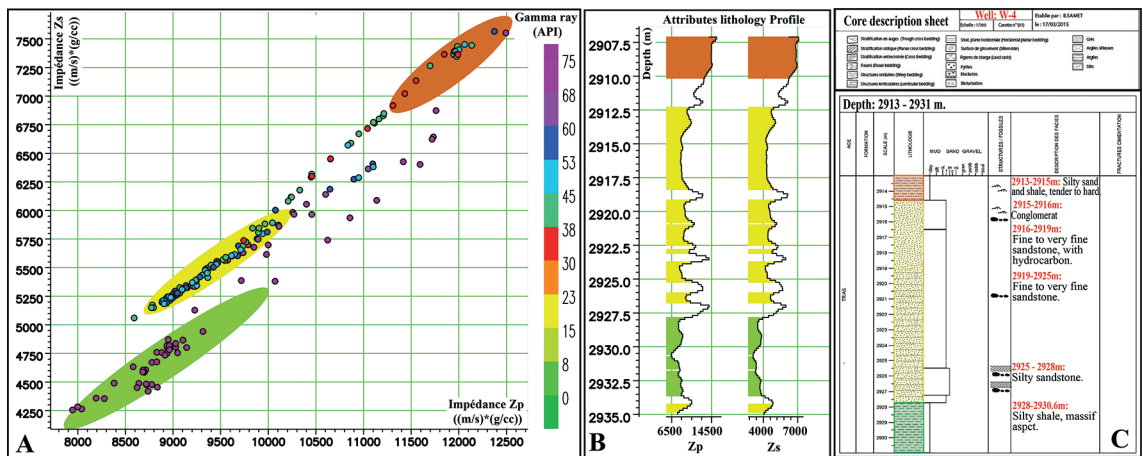


Fig. 15 - A) S-impedance versus P-impedance cross-plot over the T2 reservoir interval (2907-2935 m). B) Zp and Zs impedance logs. C) The core data description results, W-4.

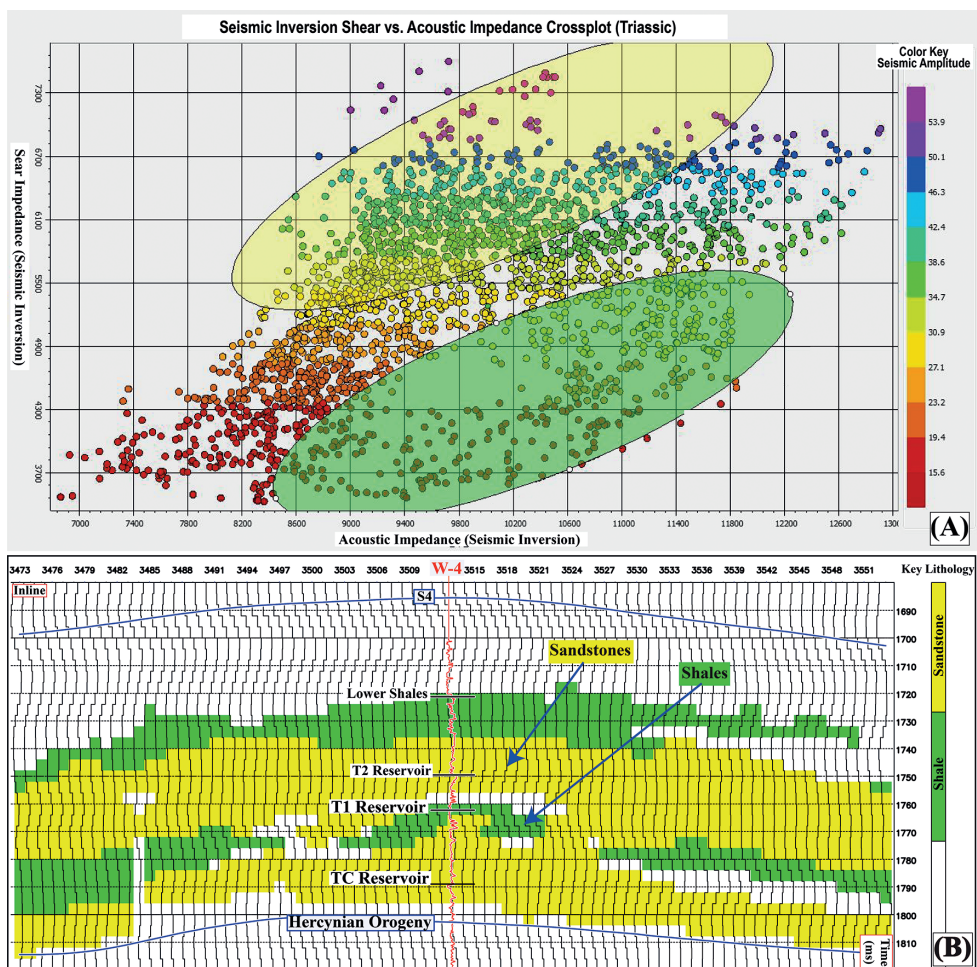


Fig. 16 - A) S-impedance versus P-impedance cross-plot using seismic inverted data over Triassic play, inlines from 3473 and 3553, time 1680-1820 ms. B) Zp and Zs impedance seismic attributes.

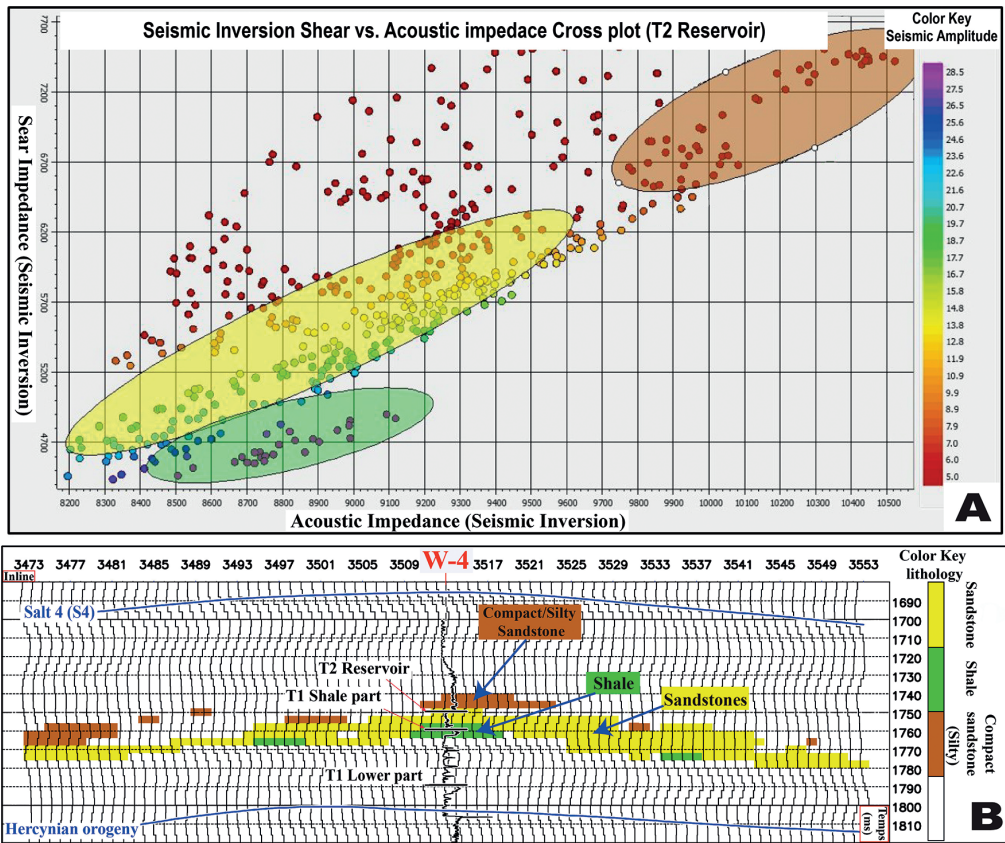


Fig. 17 - A) S-impedance versus P-impedance cross-plot using the seismic inverted data over the T2 reservoir, inlines 3473 and 3553, and time 1680-1820 ms. Three lithologies can be defined. B) The lateral distribution of sandstone, silty sandstone, and shale; the black log represents the GR log.

discrimination clustering was obtained from both seismic and well data, and well-presented in Figs. 15A, 16A, and 17A. The lateral distribution of silty sandstone in the study area does not follow a uniform continuous distribution, and it occasionally vanishes (Fig. 17B). At W-4, silty sandstone is present in the top part of the T2 reservoir (Figs. 15C and 17B).

6. Conclusions

This paper introduces a litho-discrimination approach based on petro-elastic attributes and simultaneous seismic inversion to characterise Triassic reservoirs in terms of sandstone, shale, and silty sand. The Triassic sandstone reservoirs in the Oued Mya basin, Algeria, suffer from silt contamination, which increases compaction and deteriorates the quality of the petrophysical properties.

The P-impedance versus S-impedance cross-plot has been found to be an effective tool to discriminate lithology in the study area; it exhibits a slightly linear lithology regression for sand, silt, and shale.

Seismic inversion has been used to laterally extrapolate the well data to predict how the lithology would behave far away from the well location. The adopted approach led to a better

description of shale and sandstone over the Triassic formations. Moreover, for the T2 reservoir, silty sandstone was also identified and confirmed by core data description.

It has been stated that we are dealing with a randomly distributed, non-uniform layer of silt across the T2 reservoir. The late-stage compaction (silty levels) may be the reason behind the petrophysical parameter alteration. Therefore, the distribution of the silt layer may explain the discrepancies in well performance across the area.

Finally, this study demonstrates how the litho-discrimination approach can be integrated to improve the accuracy of prospect identification and risk assessment. It also emphasises its relevance to decision-making in terms of the optimum position for prospect implementation.

In this context, the integration of well, seismic and core data using seismic inversion attributes delivers high-potential indications that can serve as reliable tools for discriminating between silt, sandstone, and shale.

Acknowledgments. We sincerely thank Sonatrach Petroleum Company for granting us access to internal studies and reports, as well as the usage of almost the data in the area of interest. We would also like to thank the University of Boumerdes, the Algerian government, the management of the Sonatrach Exploration Division, and all persons involved in this work.

REFERENCES

- Al Shekaili F., Chacko S., Serag El Din S., Yin Y., Pujol A. and Lecante G.; 2012: *Well log conditioning for quantitative seismic interpretation*. In: Abu Dhabi International Petroleum Conference and Exhibition, Abu Dhabi, UAE, SPE-161382-MS, doi: 10.2118/161382-MS.
- Amoura S., Gaci S., Barbosa S., Farfour M. and Bounif M.; 2022: *Investigation of lithological heterogeneities from velocity logs using EMD-Hölder technique combined with multifractal analysis and unsupervised statistical methods*. J. Pet. Sci. Eng., 208, 109588, doi: 10.1016/j.petrol.2021.109588.
- Anderson E., Yan J., Lubbe R., Waters K. and Pillar N.; 2008: *Log quality assessment and data correction for AVO*. In: Proc. 70th EAGE Conference and Exhibition incorporating SPE EUROPEC, European Association of Geoscientists & Engineers, Roma, Italy, 40-00288, doi: 10.3997/2214-4609.20147828.
- Arpaci T. and Ramachandran K.; 2013: *Comparison of AVO, prestack impedance inversion, and poststack impedance inversion: lithology and pore fluid discrimination in the Scotian Basin, Nova Scotia, Canada*. In: SEG Technical Program Expanded Abstracts 2013, pp. 2341-2346, doi: 10.1190/segam2013-0626.1.
- Avseth P., Mukerji T. and Mavko G.; 2005: *Quantitative seismic interpretation: applying rock physics tools to reduce interpretation risk*. Cambridge University Press, Cambridge, UK, 359 pp., doi: 10.1017/CBO9780511600074.
- Bennamane K., Amia Z. and Hamiham N.; 2016: *Potential pétrolier des unités réservoirs du Trias de la région ouest du bassin d'Oued Mya*. SONATRACH - EXPLORATION DIVISION, Hydra, Algiers, Algeria, unpublished.
- Cannon S.; 2015: *Petrophysics: a practical guide*. John Wiley & Sons Ltd., Hoboken, NJ, USA, 225 pp., doi: 10.1002/9781119117636.
- Chen T., Khaled O., Ebrahim M., Hafez M. and Mohammed I.S.; 2015: *Lithology prediction of Burgan Formation using prestack simultaneous inversion combined with statistical method: a case study in north Kuwait*. In: Expanded Abstracts, SEG Technical Program 2015, pp. 2713-2717, doi: 10.1190/segam2015-5813876.1.
- Durrani M.Z.A., Rahman S.A., Talib M., Subhani G. and Sarosh B.; 2022: *Rock physics assisted pre-stack AVA simultaneous inversion for lithofacies and porosity prediction of deeply buried mixed sedimentary reservoirs in Potwar Basin, Onshore Pakistan*. J. Appl. Geoph., 205, doi: 10.1016/j.jappgeo.2022.104766.
- Farfour M. and Foster D.; 2022: *Detection of hydrocarbon-saturated reservoirs in a challenging geological setting using AVO attributes: a case study from Poseidon field, offshore northwest region of Australia*. J. Appl. Geophys., 203, 104687, doi: 10.1016/j.jappgeo.2022.104687.
- Farfour M. and Yoon W.J.; 2014: *Ultra-thin bed reservoir interpretation using seismic attributes*. Arabian J. Sci. Eng., 39, 379-386.
- Farfour M., Yoon W.J. and Jo Y.; 2012: *Spectral decomposition in illuminating thin sand channel reservoir, Alberta, Canada*. Can. J. Pure Appl. Sci., 6, 1981-1990.

- Farfour M., Yoon W.J. and Kim J.; 2015: *Seismic attributes and acoustic impedance inversion in interpretation of complex hydrocarbon reservoirs*. J. Appl. Geoph., 114, 68-80, doi: 10.1016/j.jappgeo.2015.01.008.
- Filippova K., Kozhenkov A. and Alabushin A.; 2011: *Seismic inversion techniques: choice and benefits*. First Break, 29, 103-114, doi: 10.3997/1365-2397.29.5.49948.
- Gunarto M.O. and Irawan B.; 2010: *Well-Log conditioning and rock physics modeling: a first step in seismic reservoir characterization*. In: Proc. 34th Annual Convention & Exhibition, Indonesian Petroleum Association, Jakarta, Indonesia, IPA10-G-117.
- Hampson D.P., Russell B.H. and Bankhead B.; 2005: *Simultaneous inversion of pre-stack seismic data*. In: Expanded Abstracts, SEG Technical Program Expanded Abstracts, pp. 1633-1637, doi: 10.1190/1.2148008.
- Kalla S.; 2008: *Reservoir characterization using seismic inversion data*. Ph.D. thesis, The Craft & Hawkins Department of Petroleum Engineering, Louisiana State University, Baton Rouge, LA, USA, 152 pp.
- Mavko G., Mukerji T. and Dvorkin J.; 2020: *The rock physics handbook, 3d ed*. Cambridge University Press, Cambridge, UK, 756 pp., doi: 10.1017/9781108333016.
- Onajite E.; 2021: *Applied techniques to integrated oil and gas reservoir characterization: a problem-solution discussion with Geoscience experts*. Elsevier, Amsterdam, the Netherlands, 421 pp., doi: 10.1016/C2018-0-00421-1.
- Oyetunji O.O.; 2013: *Integrating rock physics and seismic inversion for reservoir characterization in the Gulf of Mexico*. Ph. D. thesis, Department of Earth and Atmospheric Sciences, University of Houston, Houston, U.S.A., 119 pp., <uh-ir.tdl.org/bitstream/10657/971/1/OYETUNJI-THESIS-2013.pdf>.
- Pendrel J.; 2006: *Seismic inversion-still the best tool for reservoir characterization*. CSEG Recorder, 31, 5-12.
- Russell B.H.; 1988: *Introduction to seismic inversion methods*. Society of Exploration Geophysicists, Tulsa, Oklahoma, U.S.A., 178 pp., doi: 10.1190/1.9781560802303.
- Russell B.H.; 2014: *Prestack seismic amplitude analysis: an integrated overview*. Interpretation, 2, SC19-SC36, doi: 10.1190/INT-2013-0122.1.
- Russell B. and Hampson D.; 2006: *The old and the new in seismic inversion*. CSEG Recorder, 31, 5-11.
- Sheriff R.E.; 2002: *Encyclopedic dictionary of applied geophysics. Fourth ed*. Society of Exploration Geophysicists, Tulsa, Oklahoma, U.S.A., 442 pp., doi: 10.1190/1.9781560802969.
- Simm R. and Bacon M.; 2014: *Seismic amplitude: an interpreter's handbook*. Cambridge University Press, Cambridge, UK, 281 pp., doi: 9780511984501.
- Slatt R.M.; 2006: *Stratigraphic reservoir characterization for petroleum geologists, geophysicists, and engineers*. Elsevier, Amsterdam, The Netherlands, 671 pp.
- Xu S. and Chacko S.; 2008: *Well log data conditioning using a rock physics modeling approach: examples from the Banyu Urip Field, east Java basin*. In: Proc. International Petroleum Technology Conference, Kuala Lumpur, Malaysia, IPTC-12917-MS, doi: 10.2523/IPTC-12917-MS.
- Yenwongfai H., Mondol N., Lecomte I. and Faleide J.; 2016: *Prestack simultaneous inversion to predict lithology in the Realgrunnen Subgroup of the Goliat field, SW Barents Sea*. In: Proceedings 78th EAGE Conference and Exhibition, European Association of Geoscientists & Engineers, doi: 10.3997/2214-4609.201600964.
- Zerroug S., Bounoua N. and Lounissi R., (eds) 2007: *Well Evaluation Conference Algeria 2007*. Schlumberger, Houston, TX, USA, 489 pp.
- Zrelli A., Amiri A., Barhoumi N., Bounasri M.A. and Inoubli M.H.; 2023: *Integrated seismic inversion for clastic reservoir characterization: case of the upper Silurian reservoir, Tunisian Ghadames Basin*. J. Appl. Geoph., 219, doi: 10.1016/j.jappgeo.2023.105252.

Corresponding author: Badis Zegagh
 Laboratory of Physics of the Earth (LABOPHYT), Faculty of Hydrocarbons and Chemistry,
 University of M'Hamed Bougara, Boumerdes 35000, Algeria
 Phone:+213 660130410; e-mail: b.zegagh@univ-boumerdes.dz